RSC Advances

PAPER

View Article Online
View Journal | View Issue



Cite this: *RSC Adv.*, 2020, **10**, 29910

# Gamma-radiated biochar carbon for improved supercapacitor performance†

Ezaldeen Adhamash,‡[a] Rajesh Pathak,‡[a] Qiquan Qiao,[a] Yue Zhou*[a] and Robert McTaggart*[b]

Biochar carbon YP-50 exposed to gamma radiation at 50 kGy, 100 kGy, and 150 kGy was used as an electrode for an electric double-layer capacitor. The gamma radiation affected the pore structure and pore volume of the biochar electrodes. The optimized surface morphology, pore structure, and pore volume of the biochar with an irradiation dose of 100 kGy showed outstanding specific capacitance of 246.2 F $g^{-1}$ compared to the untreated biochar (115.3 F $g^{-1}$). The irradiation dose of 100 kGy exhibited higher specific power and specific energy of 0.1 kW $kg^{-1}$ and 34.2 W h $kg^{-1}$ respectively, with a capacity retention of above 96% after 10 000 cycles at a current density of 2 A $g^{-1}$. This improvement can be attributed to the decrease in average particle size, an increase in the porosity of biochar carbon. Besides, the charge transfer resistance of supercapacitor is significantly reduced from 21.7 Ω to 7.4 Ω after treating the biochar carbon with 100 kGy gamma radiation, which implies an increase in conductivity. This gamma radiation strategy to pretreat the carbon material for improving the properties of carbon materials can be promising for the development of high-performance supercapacitors for large-scale applications.

Received 2nd July 2020
Accepted 6th August 2020

DOI: 10.1039/d0ra05764a

rsc.li/rsc-advances



## Introduction

The ever-increasing energy consumption and production largely depend on the combustion of fossil fuels, which impacts both the world economy and the environment.[1] Thus, there has been an increasing effort to develop highly efficient energy storage devices to store more energy harvested from renewable energy resources and satisfy our growing demand for energy. Electrochemical energy storage devices include two important variety groups: batteries and supercapacitors.[2,3] Batteries, which convert chemical energy to electrical energy, are used in many industrial applications such as mobile phones, computers, and vehicles, *etc.* owing to their high energy density.[4–6] However, due to their relatively low power density and the need for continuous recharging, many batteries are not suitable for all applications today. Therefore, supercapacitors that have a higher power density (>10 kW $kg^{-1}$), are lightweight, enjoy a fast charge/discharge rate, and are more stable (>$10^6$ cycles) than batteries have been developed.[4–10] Supercapacitors are appropriate for applications such as portable electronics, electric vehicles, power quality management, backup energy sources, and renewable energy applications.[8,9]

Carbon is considered as an ideal material in supercapacitors for rapid storage and release of energy because of their low cost, lightweight, mechanical and chemical stability, natural abundance, and eco-friendly. The energy storage properties of carbonaceous materials are generally attributed to electric double-layer capacitance resulting from the adsorption of ions and charged particles between the electrode and the electrolyte. To further increase the specific capacitance of supercapacitors, carbon materials should be activated for increasing the specific surface area (SSA), porosity, and conductivity before using them as electrodes. Currently, physical and chemical activation are the primary methods used in the manufacture of electrode materials.[10] Carbon precursor grains get partial controlled oxidation by these activation methods, leading to a higher surface area and the widening of the existing porous resulting in higher porosity.[11–13] Physical activation uses gases such as $CO_2$ or $H_2$ under high temperatures to develop the porosity of electrode material. These gases react with carbon atoms to create carbon monoxide, leading to a change in the structure of the materials.[13–15] Chemical activation develops the carbon material under high temperature to enhance reactions between carbon atoms and the activation reagents such as zinc chloride, phosphoric acid, or potassium hydroxide. With this kind of activation, the pore size could be more controlled than physical activation.[16–19]

[a]*Department of Electrical Engineering and Computer Science, South Dakota State University, Brookings, SD 57007, USA. E-mail: yue.zhou@sdstate.edu*

[b]*Department of Physics, South Dakota State University, Brookings, SD 57007, USA. E-mail: robert.mctaggart@sdstate.edu*

† Electronic supplementary information (ESI) available. See DOI: 10.1039/d0ra05764a

‡ These authors equally contributed to this work.

Recently, the effect of irradiation in supercapacitor materials has been a field of great interest.[20] In many early studies of particle irradiation, the subject of treatment and modification of carbon materials has been a very popular topic. For example, several experiments showed that carbon materials can be modified by electron and high energy photon irradiation to change their mechanical, electronic, and magnetic properties.[21] In contrast, gamma radiation can be used as a promising method for fabrication, modification, and manipulation of carbon materials.[22] The optimized gamma irradiation technique increases the specific capacitance due to an increase in specific surface area (SSA), high pore volume, high defects, and improvement in the conductivity *i.e.* fast charge transfer. Another reason behind choosing gamma radiation to treat carbon materials was the fact that it's a safe method that could protect the environment against pollution, reduce maintenance costs and save energy consumption.[22,23]

Ahmed Reza *et al.* in 2019 used different radiation doses from 0 to 100 kGy (1 kGy = 1000 gray = 1000 joule $kg^{-1}$) of gamma-rays (*i.e.* γ-irradiation) to treat carbon nanostructure materials (CNMs) including graphene nanoplate, graphene oxide, single-walled carbon nanotube (SWCNT) and multi-walled carbon nanotubes (MWCNT). All materials showed that there was a simultaneous competition between new defects and graphitization in the CNMs depending on the gamma dose and the kind of material.[22] Raman spectroscopy for SWCNT showed that the value of $I_D/I_G$ (the disorder peak and graphitic peak ratio) increased with the increase of radiation doses.[22] In 2015 Najah *et al.* used gamma irradiations of 5 kGy, 15 kGy, and 20 kGy to treat and activate green monoliths (GMs) and use them as electrodes for supercapacitor. The specific capacitance increased from 121 F $g^{-1}$ to 196 F $g^{-1}$ after 5 kGy γ radiations and then decreased to be 11 F $g^{-1}$, 12 F $g^{-1}$ when γ radiation increased to 15, 20 kGy. The irradiation dose of 5 kGy appears to be a suitable dose for GMs supercapacitor and produces a specific power and specific energy of 236 W $kg^{-1}$ and 5.45 W h $kg^{-1}$.[24] In another recent study, Ankamwar *et al.* compared graphene-gold nanocomposites fabricated by chemical and γ-irradiation methods as an electrode for supercapacitors. The specific capacitance value was 5 times greater with γ-irradiation than with the chemical synthesized electrode. In addition, life cycle testing demonstrated that electrodes subjected to γ-rays have a suitably long cycle life and a stable specific capacitance after 600 cycles.[25,26] The main shortcoming of the most previous works is that they focus on how to improve the properties of the pore structure and surface chemistry of carbon materials by gamma radiation without using them as electrodes of supercapacitors. However, to the best of our knowledge, only a few reports exist on radiation effects on supercapacitor electrodes.[27]

With these considerations in mind, we report the use of a gamma radiation technique to treat and modify the properties of biochar carbon YP-50 and use the treated carbon as an electrode for supercapacitors. The optimized dose of 100 kGy demonstrated showed outstanding specific capacitance of 246.2 F $g^{-1}$ compared to the untreated biochar (115.3 F $g^{-1}$), the high specific power of 0.1 kW $kg^{-1}$ and specific energy of 34.2 W h $kg^{-1}$ with a capacity retention of above 96% after 10 000 cycles at a current density of 2 A $g^{-1}$. This improvement can be attributed to the high SSA (*i.e.* decrease in average particle size), increase in the porosity of biochar carbon, and increase in the conductivity (*i.e.* decrease in the charge transfer resistance ($R_{ct}$) from 21.7 Ω without treatment to 7.4 Ω) with 100 kGy gamma radiation.

## Experimental details

### Treatment with gamma radiation

An industrial gamma sterilizer operated by the 3M Corporation was used to irradiate biochar. The facility uses gamma rays of energies 1173 keV and 1332 keV that are generated during the radioactive decay of cobalt-60, where 1 keV is 1000 eV and 1 eV is the energy gained by an electron in passing through a voltage of 1 volt. Usually, the sample is in a tote that lies on a track running next to the source. The facility has been used to study the mechanical effects of gamma irradiation on other materials besides biochar, such as samples of high-density polyethylene (HDPE),[28] Acrylonitrile Butadiene Styrene (ABS),[29] and 3d-printed polylactic acid (PLA)[30] that may be used in various engineering applications. Fig. 1 shows a simple explanation about the gamma process to treat a sample. Radiation doses from an industrial gamma sterilizer can be measured both by physical dosimeters and by Monte Carlo simulations that model the energy deposited by the radiation in the sample.[31,32] Radiation doses are measured in units of grays, where one gray (Gy) is a joule absorbed per kilogram of material, and 1 kilogray (1 kGy) is 1000 Gy.

As chemical bonds are broken during irradiation, free radicals and new internal bonding structures may occur due to chain scission, crosslinking, and one of many oxidative effects.[33] It should be noted that irradiations in the present study occurred in the presence of air. In addition to the surrounding carbon atoms, bonds had access to oxygen and hydrogen in the air. One alternative to reduce or avoid such effects would be to immerse the sample in pure nitrogen. While these gamma rays will break chemical bonds, they lack the energy to displace protons or neutrons from nuclei. Thus, an irradiated sample does not become radioactive. In the current effort, we investigate the effects of gamma-ray irradiation upon

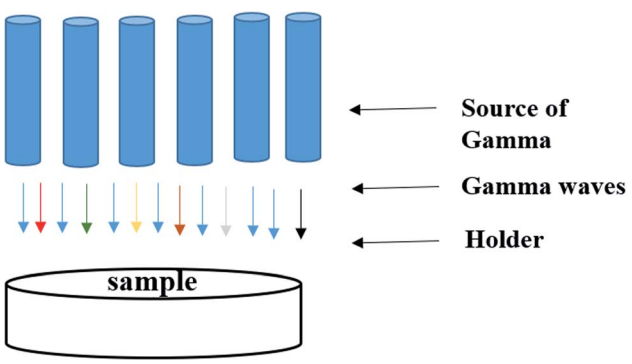


Fig. 1 Schematic of the gamma radiation process at 3M Corporation.

an activated carbon powder (YP-50 from Kuraray chemicals, derived from coconut shell and activated by steam) and its resulting use as the electrode material for EDLCs. The doses applied were 50 kGy, 100 kGy, and 150 kGy, respectively. The objective of this study was to improve the properties of the carbon material and increase the performance of supercapacitors fabricated with said material.

### Electrode preparation

The weight ratio of 8 : 1 : 1 for activated carbon, ethyl cellulose, and acetylene black were mixed using 80 ml of isopropyl alcohol (IPA) as a solvent to make a slurry. The solution was then ultrasonicated for 60 minutes and stirred for 30 minutes using a magnetic stirrer. A dimension of 2.5 cm × 2.5 cm of nickel foil from Alfa Aesar was used as a metal substrate for electrophoretic deposition. 3M scotch tape was used to cover the backside to avoid any deposition on it and dipped into the carbon solution with the copper foil (as a counter electrode) of the same dimension of nickel foil for 10 minutes. Around 1.5 cm was the distance between the two electrodes. The DC voltage was at 80 V with 0.16 ampere. After 10 min of deposition, the electrodes were kept in the vacuum overnight at 100 °C. The Ni electrodes were cut into a circular shape of 15 mm by using an MTI precision disk cutter (MSK-T-06) where the active mass of carbon was 4 mg. The two pieces of tissues, as a separator, were cut into a diameter of 16 mm and dipped for 15 minutes in 6 mol $L^{-1}$ KOH electrolyte.

### Structural characterization

The Brunauer–Emmett–Teller (BET) tests Micromeritics – ASAP 2020 was used to calculate the SSA, the pore size distribution, and the pore volume. Hitachi S3400-N scanning electron microscope (SEM) was used to investigate the structure and the surface morphology of the carbon before and after the treatments. The Raman spectra (LabRam HR800) at room temperature, with an excitation wavelength of 532 nm from a diode-pumped solid-state laser was used to characterize the structure of biochar.

### Electrochemical characterizations

The cyclic voltammetry (CV) measurement was carried out by an electrochemical workstation (Ametek VERSATAT-450 potentiostat) at the scan rate of 10 mV $s^{-1}$. The electrochemical impedance spectroscopy (EIS) measurement was conducted by an electrochemical workstation (Ametek VERSATAT-450 potentiostat) at an applied voltage of 10 mV within a frequency range of 100 kHz to 0.1 Hz. The galvanostatic charge/discharge (GCD) measurement was conducted using the Neware battery analyzer cycling between 0.0 V to 1.0 V at a current density of 2 A $g^{-1}$. The specific capacitance (SC) was calculated from the relationship between the potential and elapsed time and using the following equation,

$$\mathrm{SC} = \frac{4I\mathrm{d}t}{m\mathrm{d}v} \quad (1)$$

where SC is the specific capacitance (F $g^{-1}$), $I$ is the charge or discharge current density, d$t$ is the charge or discharge time, $m$ is the total mass of active material on both electrodes, and d$v$ is the change during discharge in voltage. The energy density and power density were calculated using the two formulas.

$$E = \frac{1}{2}\left(C\Delta V^2\right)\ \left(\mathrm{W\ h\ kg^{-1}}\right) \quad (2)$$

$$P = \frac{E \times 3.6}{\Delta t}\ \left(\mathrm{kW\ kg^{-1}}\right) \quad (3)$$

where $E$ is the energy density, SC is the specific capacitance of both electrodes, $P$ is the power density.

## Result and discussion

The morphological studies of the carbon treated by gamma rays are carried out by scanning electron microscopy (SEM). The SEM image of the untreated sample shows that the biochar contained a mixture of large and small particles (Fig. 2a). Following the 50 kGy radiation, the average particle size seems to be smaller without any significant changes (Fig. 2b). For 100 kGy radiation, the average particle size of the biochar sample is drastically lowered. Besides, smaller particle size offers a large surface area and ensures better accessibility to the electrolyte. The connectivity between the grains of the particles is still maintained with the decrease of particles' average size, which enhances the electrical conductivity and specific surface (Fig. 2c). These results implied that the gamma radiation etched off and broke down certain phases in the biochar YP-50. The 150 kGy broke down the large particles into extremely fine and smaller particles (Fig. 2d).[34] This can break the connectivity between the particles, which lowers the defects and disorder, and interconnection among the particles, resulting in lower electrical conductivity. The insufficient particle size and reduced conductivity lead to a lower total capacitance due to sluggish charge transport.[35]

To investigate the porosity, and SSA of gamma radiation on the biochar YP-50, Brunauer–Emmett–Teller (BET)

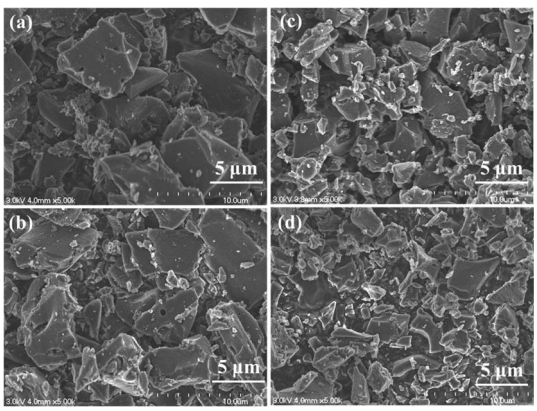


Fig. 2 SEM images of (a) untreated biochar, (b) 50 kGy gamma activated, (c) 100 kGy gamma activated, and (d) 150 kGy gamma activated biochar.

 

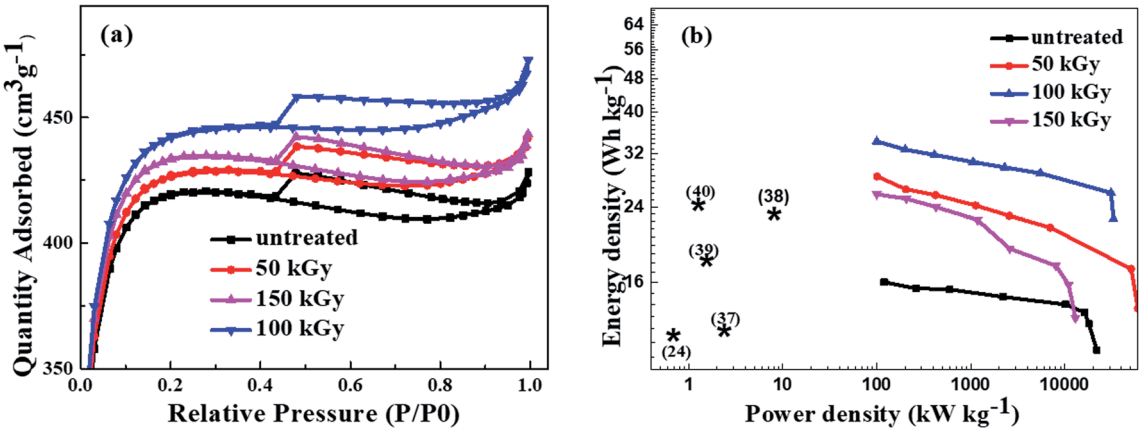


Fig. 3 (a) Nitrogen adsorption–desorption isotherms for activated biochar from non-irradiated and γ-irradiated at different gamma radiation dosage. (b) Ragone plot for untreated, 50 kGy, 100 kGy, and 150 kGy gamma radiation.

measurement is carried out. Fig. 3a shows the $N_2$ sorption isotherms of untreated, 50 kGy, 100 kGy, and 150 kGy gamma irradiation of biochar YP-50. The carbon samples before and after gamma radiation have shown a very similar type IV isotherms curve.

Clear hysteresis loops in the relative pressure range between 0.4–0.9 a sharp capillary condensation in the relative pressure range from 0.9–1.0 are observed, indicating a regular mesoporous structure.[36] The BET measurement shows that the untreated sample has the smallest pore volume and surface area of 0.46 $cm^3\ g^{-1}$, 1451.2 $m^2\ g^{-1}$ respectively. After 50 kGy doses, its plot was overlapped with a 150 kGy plot with similar values of surface area and pore volume. The reason behind that is 50 kGy is not enough dose to break down the chemical bonds and 150 kGy was large enough to break all the bigger particles into smaller ones. 100 kGy dose has the largest volume and surface area contributions from mesoporous particles, which are important for electrolyte ions to transport during charging and discharging. All the results from the BET measurements are summarized in Table 1. Fig. 3b shows the Ragone plot (power density *vs.* energy density based on the total mass of the active material on both electrodes) of the supercapacitor made of untreated and treated carbon with 50 kGy, 100 kGy, and 150 kGy gamma rays. The highest energy density of 34.2 W h $kg^{-1}$ at the specific power of 0.1 kW $kg^{-1}$ is obtained from carbon treated with 100 kGy of gamma irradiation. The supercapacitor from carbon treated with 100 kGy displays an excellent performance, even when the power density of the device reaches 33 kW $kg^{-1}$, the energy density remains 22.5 W h $kg^{-1}$, which shows that this method of treatment is a promising way to fabricate commercial supercapacitors. The calculated values of energy density and power density at different current density are summarized in Table S1 (ESI†). The calculated energy density and power density in this work is higher than or comparable to a few reported electric double layer capacitor devices[24,37–40] as compared in Table S2.† Fig. S1† shows the Raman spectroscopy of untreated, 50 kGy, 100 kGy, and 150 kGy of gamma radiation. The characteristic peak around 1600 $cm^{-1}$ (G-band) corresponded to individual graphite dominated by $sp^2$ bonds, while the peak around 1340 $cm^{-1}$ (D-band) indicated an imperfect structure of carbon.[5,24,41,42] Table S3† shows the ratio of $I_D/I_G$ for untreated carbon, treated carbon with 50 kGy, 100 kGy, and 150 kGy gamma radiation. The untreated carbon shows the $I_D/I_G$ ratio of 0.833. In contrast, the treated carbon with a dose of 100 kGy shows the highest value of the $I_D/I_G$ ratio of 0.843 implying the creation of more defects. This phenomenon can be explained as that gamma radiation confirmed defects due to the heating caused by its rays at high doses near to 100 kGy. Irradiation of the carbon with energetic gamma-rays leads to the creation of atomic defects in the materials.[22]

Cyclic voltammetric (CV) measurement is carried out to characterize the properties of supercapacitor based on the various carbon samples. Fig. 4a shows that all samples exhibited a rectangular shape over a potential range of 0.0 to 1.0 V at

Table 1 The BET and pore structure parameters of the untreated and treated samples

| Samples | $S_{BET}$[a]/$m^2\ g^{-1}$ | T-micropore volume[b]/$cm^3\ g^{-1}$ | Average pore width/nm |
|---|---|---|---|
| Untreated sample | 1451.2 | 0.46 | 1.74 |
| 50 kGy | 1507.9 | 0.52 | 1.77 |
| 100 kGy | 1562.9 | 0.55 | 1.82 |
| 150 kGy | 1511.1 | 0.53 | 1.75 |

[a] SSA from multiple BET method. [b] Total micropore volume at $P/P_0 = 0.99$.

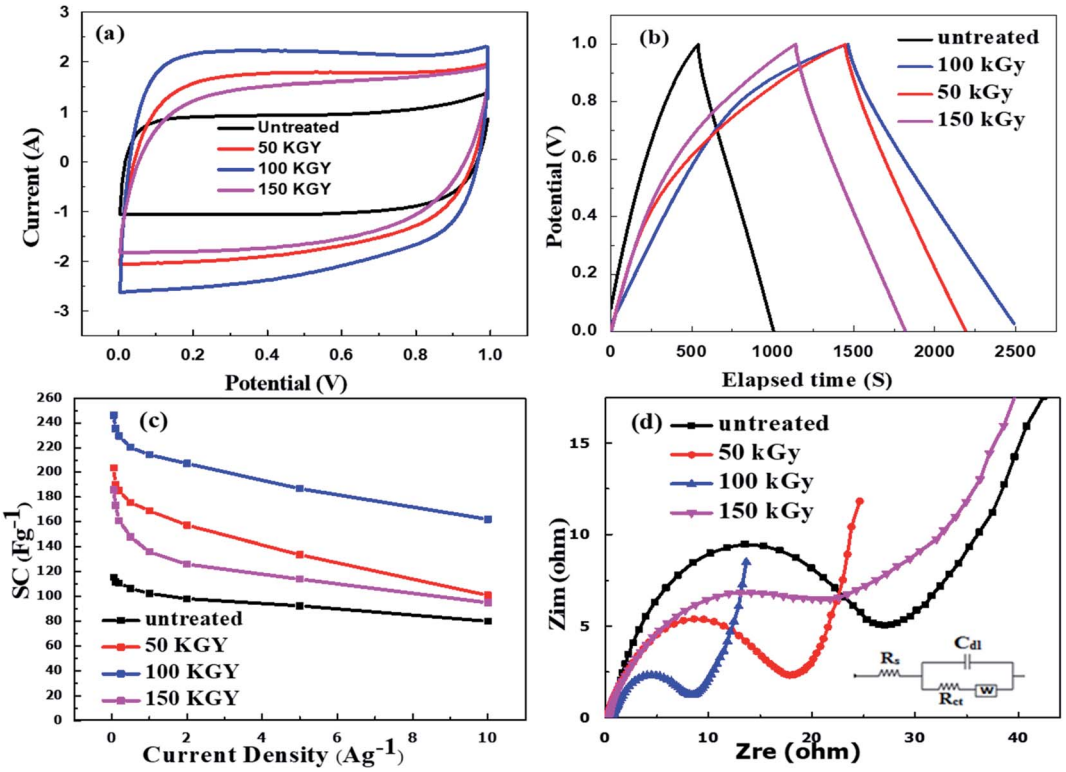


Fig. 4 The electrochemical properties were tested using a two-electrode system. (a) CV curves of untreated, 50 kGy, 100 kGy, and 150 kGy gamma radiation electrodes with a scan rate of 10 mV $s^{-1}$, (b) galvanostatic charge–discharge curve of untreated, 50 kGy, 100 kGy, and 150 kGy gamma radiation electrodes at 0.05 A $g^{-1}$, and (c) the specific capacitance as a function of current density for untreated, 50 kGy, 100 kGy, and 150 kGy gamma radiation electrodes electrode, and (d) EIS curves of untreated, 50 kGy, 100 kGy, and 150 kGy gamma radiation electrodes at an applied voltage of 10 mV within a frequency range of 100 kHz to 0.1 Hz.

a sweep rate of 10 mV $s^{-1}$ indicating an electric double layer capacitance behavior. The carbon treated with 100 kGy showed the best rectangular shape. Fig. 4b shows the galvanostatic charge–discharge plots of untreated, 50 kGy, 100 kGy, and 150 kGy gamma radiation treatments carbon electrode at 0.05 A $g^{-1}$ in the voltage window of 0.0–1.0 V. The triangular shapes of plots indicate the electrodes have good capacitive behavior. The specific capacitance obtained was 115.3, 203.6, 246.2, and 185.0 F $g^{-1}$ for untreated and treated carbon with 50, 100, and 150 kGy doses, respectively. The specific capacitance of all the electrodes was calculated at various current densities. As can be seen in Table S4.† Fig. 4c, the specific capacitance decreases gradually with the increase of current density, which can be attributed to the limited transportation of the electrolyte ions. The carbon treated with 100 kGy shows the highest capacitance of 162.0 F $g^{-1}$ even at a high current density of 10 A $g^{-1}$ compared to all other samples. These results indicate that good rate capability, and also, suggests the ability of the carbon treated with gamma radiation to deliver high power. The high capacitance and excellent rate performance are due to the stringy morphology of the carbon electrodes after gamma treatments, which allow the fast transportation of the electrolyte and efficient ion diffusion.[43]

To investigate the charge transfer behavior of the supercapacitor, electrochemical impedance spectroscopy (EIS) is carried out. Typical Nyquist impedance spectra recorded for untreated, 50 kGy, 100 kGy, and 150 kGy gamma radiation is shown in Fig. 4d. There is no significant difference in the series resistance ($R_s$) among all four samples due to the identical method of supercapacitor fabrication. However, the carbon treated with 100 kGy gamma shows the least charge transfer resistance ($R_{ct}$) of 7.4 Ω compared to other samples. The lower $R_{ct}$ of carbon treated with 100 kGy gamma can be attributed to the high surface area and high porosity, and smaller particle size morphology of the carbon electrodes, which allow the fast transportation of the electrolyte and efficient ion diffusion.[43,44] All the impedance results are summarized in Table S5.†

To further investigate the excellent electrochemical performances of biochar carbon under gamma irradiation, most of the measurements are repeated after 10 000 cycles. For example, the CV measurement of all the samples after 10 000 cycles (Fig. S2a†) shows a similar rectangular shape as in (Fig. 4a), implying stability of the electrodes. The carbon treated with 100 kGy shows the highest capacity retention of ~97% after 10 000 cycles at current density 2 A $g^{-1}$ demonstrating its excellent cycling stability. 50 kGy shows ~93% after 10 000 cycles comparing to the 150 kGy which shows ~88% and untreated sample which shows ~83% (Fig. S2b†). However, the EIS measurement (Fig. S2c†) carried out after 10 000 cycles for all the samples show the typical similar curve as in Fig. 4d. Also,

 

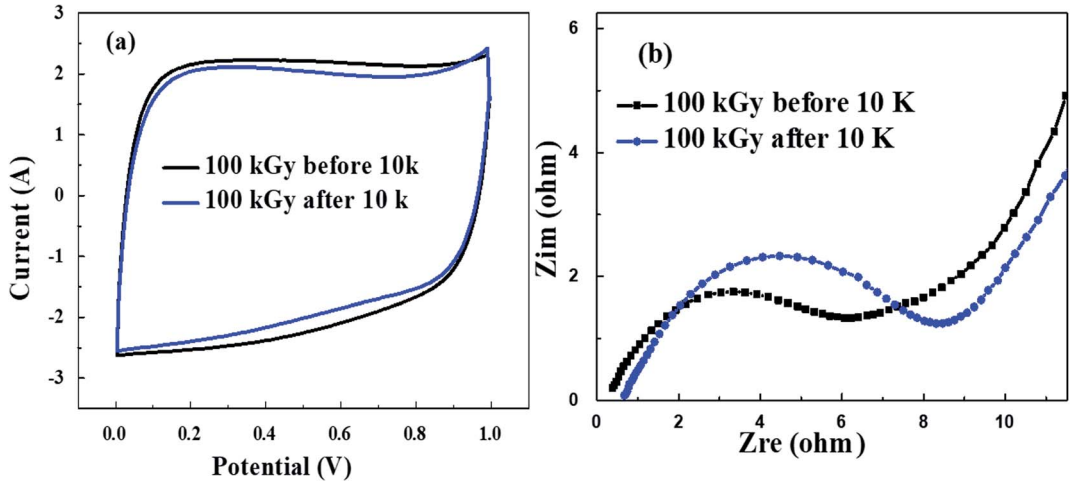


Fig. 5 (a) CV before and after 10 000 cycles for 100 kGy and (b) EIS before and after 10 000 cycles for 100 kGy.

Fig. S2c† shows that the 100 kGy sample still has the lowest $R_{ct}$ and the untreated sample has the highest $R_{ct}$ which implies the highest cycling stability of 100 kGy treated carbon. The galvanostatic charge/discharge (GCD) longer cycling test is performed after 10 000 cycles at a current density of 2 A $g^{-1}$ (Fig. S2d†), in this figure the 100 kGy sample still has the highest elapsed time value compared to 50, 150 kGy and untreated samples which indicated that 100 kGy has good capacitive behavior. To have a complete picture of the electrochemical behavior of supercapacitors after 100 kGy gamma radiation, the CV and EIS after 10 000 cycles should be compared to the same measurements before, where the number of cycles was 10 cycles as shown in Fig. 5a and b. Where the CV and EIS for 100 kGy before and after have the same rectangular shape and insignificant change in $R_{ct}$, which indicated the electrochemical stability after 10 000 cycles. These all results indicated that even after 10 000 cycles the device still works very well so this method is suitable to improve the electrochemical performance of the electro double layer capacitor based on carbon materials by improving their specific capacitance, energy density, power density, rate capability and/or cyclic stability.

## Conclusion

In summary, the carbon YP-50 is activated by a novel and efficient way of treating the carbon with different doses of gamma radiation. The gamma radiation breaks the chemical bond and decreases the particle size thereby increasing the SSA. As a result, the carbon treated with 100 kGy gamma rays shows an increase in specific capacitance from 115.3 F $g^{-1}$ (untreated) to 246.2 F $g^{-1}$ and the highest capacity retention of ~97%. Besides, the carbon treated with 100 kGy gamma exhibits a high energy density of 34.2 W h $kg^{-1}$, the power density of 0.1 kW $kg^{-1}$ at density current of 0.05 A $g^{-1}$. Our investigation in this work not only opens up and provides a novel guideline to engineer gamma treatments into a promising electro double layer capacitor material, but also presents a suitable and affordable general method to treat and activate electrodes materials for devices.

## Conflicts of interest

The authors declare no competing interests.

## Acknowledgements

This work has been supported by USDA North Central Sun Grant, SDBoR Competitive Grant Program, NSF MRI (1428992), NASA EPSCoR (NNX15AM83A), SDBoR R&D Program, and EDA University Center Program (ED18DEN3030025).

## References

1 S. Deutz, *et al.*, Cleaner production of cleaner fuels: wind-to-wheel–environmental assessment of CO 2-based oxymethylene ether as a drop-in fuel, *Energy Environ. Sci.*, 2018, **11**(2), 331–343.
2 T. Mehtab, *et al.*, Metal–organic frameworks for energy storage devices: batteries and supercapacitors, *J. Energy Storage*, 2019, **21**, 632–646.
3 N. S. Punde, A. S. Rajpurohit and A. K. Srivastava, Fabrication of an Advanced Symmetric Supercapattery Based on Nanostructured Bismuth-Cobalt-Zinc Ternary Oxide Anchored on Silicon Carbide Hybrid Composite Electrode, *Energy Technol.*, 2019, **7**(9), 1900387.
4 R. Pathak, *et al.*, Fluorinated hybrid solid-electrolyte-interphase for dendrite-free lithium deposition, *Nat. Commun.*, 2020, **11**(1), 1–10.
5 R. Pathak, *et al.*, Ultrathin bilayer of graphite/$SiO_2$ as solid interface for reviving Li metal anode, *Adv. Energy Mater.*, 2019, **9**(36), 1901486.
6 R. Pathak, Y. Zhou and Q. Qiao, Recent Advances in Lithiophilic Porous Framework toward Dendrite-Free Lithium Metal Anode, *Appl. Sci.*, 2020, **10**(12), 4185.

7 E. Kim, *et al.*, Etching-Assisted Crumpled Graphene Wrapped Spiky Iron Oxide Particles for High-Performance Li-Ion Hybrid Supercapacitor, *Small*, 2018, **14**(16), 1704209.
8 J. Bae, M. K. Song, Y. J. Park, J. M. Kim, M. Liu and Z. L. Wang, Fiber supercapacitors made of nanowire-fiber hybrid structures for wearable/flexible energy storage, *Angew. Chem., Int. Ed.*, 2011, **50**(7), 1683–1687.
9 S. H. Wang, *et al.*, Stable Li metal anodes *via* regulating lithium plating/stripping in vertically aligned microchannels, *Adv. Mater.*, 2017, **29**(40), 1703729.
10 H. N. Tran, H.-P. Chao and S.-J. You, Activated carbons from golden shower upon different chemical activation methods: synthesis and characterizations, *Adsorpt. Sci. Technol.*, 2018, **36**(1–2), 95–113.
11 L. L. Zhang and X. Zhao, Carbon-based materials as supercapacitor electrodes, *Chem. Soc. Rev.*, 2009, **38**(9), 2520–2531.
12 A. Pandolfo and A. Hollenkamp, Carbon properties and their role in supercapacitors, *J. Power Sources*, 2006, **157**(1), 11–27.
13 B. Xu, *et al.*, What is the choice for supercapacitors: graphene or graphene oxide?, *Energy Environ. Sci.*, 2011, **4**(8), 2826–2830.
14 A. Albiniak, D. Bégin, E. Alain, G. Furdin, E. Broniek and J. Kaczmarczyk, Effect of iron enrichment with GIC or $FeCl_3$ on the pore structure and reactivity of coking coal, *Fuel*, 1997, **76**(14–15), 1383–1387.
15 P. Simon and Y. Gogotsi, Materials for electrochemical capacitors, in *Nanoscience And Technology: A Collection of Reviews from Nature Journals*, World Scientific, 2010, pp. 320–329.
16 F. Hofmann, C. Ferracin, G. Marsh and R. Dumas, Influenza vaccination of healthcare workers: a literature review of attitudes and beliefs, *Infection*, 2006, **34**(3), 142–147.
17 C. Almansa, M. Molina-Sabio and F. Rodríguez-Reinoso, Adsorption of methane into $ZnCl_2$-activated carbon derived discs, *Microporous Mesoporous Mater.*, 2004, **76**(1–3), 185–191.
18 Y. Zhai, Y. Dou, D. Zhao, P. F. Fulvio, R. T. Mayes and S. Dai, Carbon materials for chemical capacitive energy storage, *Adv. Mater.*, 2011, **23**(42), 4828–4850.
19 A. R. Mohamed, M. Mohammadi and G. N. Darzi, Preparation of carbon molecular sieve from lignocellulosic biomass: a review, *Renewable Sustainable Energy Rev.*, 2010, **14**(6), 1591–1599.
20 F. Banhart, Irradiation effects in carbon nanostructures, *Rep. Prog. Phys.*, 1999, **62**(8), 1181.
21 A. Krasheninnikov and K. Nordlund, Ion and electron irradiation-induced effects in nanostructured materials, *J. Appl. Phys.*, 2010, **107**(7), 3.
22 A. R. Vatankhah, M. A. Hosseini and S. Malekie, The characterization of gamma-irradiated carbon-nanostructured materials carried out using a multi-analytical approach including Raman spectroscopy, *Appl. Surf. Sci.*, 2019, **488**, 671–680.
23 Z. Xu, *et al.*, Nano-structure and property transformations of carbon systems under γ-ray irradiation: a review, *RSC Adv.*, 2013, **3**(27), 10579–10597.
24 N. S. M. Nor, *et al.*, Influence of gamma irradiation exposure on the performance of supercapacitor electrodes made from oil palm empty fruit bunches, *Energy*, 2015, **79**, 183–194.
25 B. Ankamwar, P. Das and U. Sur, Graphene–gold nanoparticle-based nanocomposites as an electrode material in supercapacitors, *Indian J. Phys.*, 2016, **90**(4), 391–397.
26 S. M. Ghoreishian, *et al.*, γ-radiolysis as a highly efficient green approach to the synthesis of metal nanoclusters: a review of mechanisms and applications, *Chem. Eng. J.*, 2019, **360**, 1390–1406.
27 F. Barzegar, A. Bello, D. Y. Momodu, N. Manyala and X. Xia, Effect of radiation on the performance of activated carbon base supercapacitor: Part I. Influence of microwave irradiation exposure on electrodes material, *Energy Procedia*, 2019, **158**, 4554–4559.
28 C. West, R. McTaggart, T. Letcher, D. Raynie and R. Roy, Effects of Gamma Irradiation Upon the Mechanical and Chemical Properties of 3D-Printed Samples of Polylactic Acid, *J. Manuf. Sci. Eng.*, 2019, **141**(4), 041002.
29 B. Rankouhi, S. Javadpour, F. Delfanian, R. McTaggart and T. Letcher, Experimental Investigation of Mechanical Performance and Printability of Gamma-Irradiated Additively Manufactured ABS, *J. Mater. Eng. Perform.*, 2018, **27**(7), 3643–3654.
30 J. Cassidy, S. Nesaei, R. McTaggart and F. Delfanian, Mechanical response of high density polyethylene to gamma radiation from a Cobalt-60 irradiator, *Polym. Test.*, 2016, **52**, 111–116.
31 M. Bailey, J. Sephton and P. Sharpe, Monte Carlo modelling and real-time dosemeter measurements of dose rate distribution at a $^{60}Co$ industrial irradiation plant, *Radiat. Phys. Chem.*, 2009, **78**(7–8), 453–456.
32 D. E. Weiss and R. J. Stangeland, Dose prediction and process optimization in a gamma sterilization facility using 3-D Monte Carlo code, *Radiat. Phys. Chem.*, 2003, **68**(6), 947–958.
33 K. A. Walker, L. J. Markoski, G. A. Deeter, G. E. Spilman, D. C. Martin and J. S. Moore, Crosslinking chemistry for high-performance polymer networks, *Polymer*, 1994, **35**(23), 5012–5017.
34 R. K. Gupta, M. Dubey, P. Kharel, Z. Gu and Q. H. Fan, Biochar activated by oxygen plasma for supercapacitors, *J. Power Sources*, 2015, **274**, 1300–1305.
35 C. Portet, G. Yushin and Y. Gogotsi, Effect of carbon particle size on electrochemical performance of EDLC, *J. Electrochem. Soc.*, 2008, **155**(7), A531.
36 W. Huang, H. Zhang, Y. Huang, W. Wang and S. Wei, Hierarchical porous carbon obtained from animal bone and evaluation in electric double-layer capacitors, *Carbon*, 2011, **49**(3), 838–843.
37 W. Yang, W. Yang, F. Ding, L. Sang, Z. Ma and G. Shao, Template-free synthesis of ultrathin porous carbon shell with excellent conductivity for high-rate supercapacitors, *Carbon*, 2017, **111**, 419–427.
38 K. Jayaramulu, *et al.*, Ultrathin hierarchical porous carbon nanosheets for high-performance supercapacitors and

 

redox electrolyte energy storage, *Adv. Mater.*, 2018, **30**(15), 1705789.

39 I. I. Misnon, N. K. M. Zain and R. Jose, Conversion of oil palm kernel shell biomass to activated carbon for supercapacitor electrode application, *Waste Biomass Valorization*, 2019, **10**(6), 1731–1740.

40 L. Yuan, *et al.*, Flexible solid-state supercapacitors based on carbon nanoparticles/$MnO_2$ nanorods hybrid structure, *ACS Nano*, 2011, **6**(1), 656–661.

41 X. Wen, D. Zhang, T. Yan, J. Zhang and L. Shi, Three-dimensional graphene-based hierarchically porous carbon composites prepared by a dual-template strategy for capacitive deionization, *J. Mater. Chem. A*, 2013, **1**(39), 12334–12344.

42 O. Paris, C. Zollfrank and G. A. Zickler, Decomposition and carbonisation of wood biopolymers—a microstructural study of softwood pyrolysis, *Carbon*, 2005, **43**(1), 53–66.

43 D. Kalpana, S. Cho, S. Lee, Y. Lee, R. Misra and N. Renganathan, Recycled waste paper—A new source of raw material for electric double-layer capacitors, *J. Power Sources*, 2009, **190**(2), 587–591.

44 R. Pathak, *et al.*, Self-recovery in Li-metal hybrid lithium-ion batteries *via* WO 3 reduction, *Nanoscale*, 2018, **10**(34), 15956–15966.